PHYSICAL REVIEW E **68**, 020401(R) (2003)

Diffusion-limited aggregation in channel geometry

Ellák Somfai* and Robin C. Ball
Department of Physics, University of Warwick, Coventry CV4 7AL, United Kingdom

Jason P. DeVita and Leonard M. Sander
Michigan Center for Theoretical Physics, Department of Physics, University of Michigan, Ann Arbor, Michigan 48109-1120, USA
(Received 22 April 2003; published 29 August 2003)

We performed extensive numerical simulation of diffusion-limited aggregation in two-dimensional channel geometry. Contrary to earlier claims, the measured fractal dimension $D=1.712\pm0.002$ and its leading correction to scaling are the same as in the radial case. The average cluster, defined as the average conformal map, is similar but not identical to Saffman-Taylor fingers.

DOI: 10.1103/PhysRevE.68.020401 PACS number(s): 61.43.Hv

Diffusion-limited aggregation (DLA) has attracted considerable attention since its introduction by Witten and Sander in 1981 [1]. In this model an aggregate or cluster grows by capturing diffusing particles which irreversibly attach to it on first contact. This is the discrete model of a wide variety of physical systems in the Laplacian growth class. This class can be modeled with a field, satisfying the Laplace equation outside of a growing cluster, where the cluster grows in proportion to the gradient of the field at the boundary. A generalization of DLA, known as the dielectric breakdown model (DBM) [2], allows growth proportional to the field gradient to the exponent η. DLA is regained for $\eta=1$. The majority of our current knowledge about DLA is numerical (mostly in two dimensions and radial geometry), although progress has been made in the theoretical front as well (see, e.g., Refs. [3,4]).

One of the controversies surrounding DLA in channel geometry has been that the fractal dimension might differ from that in the radial case. This claim has been based on small size simulations [5–7] or small size calculations [8,9]. In this paper, based on extensive numerical simulations of off-lattice DLA in channel, we show that the fractal dimension is asymptotically the *same* in the two geometries.

One of the most important differences between the two geometries is that for the channel the continuum version of the problem (Laplacian growth) has a stable solution without tip splitting instability and finger competition. These stationary translating solutions—called Saffman-Taylor fingers [10]—have been studied in viscous fingering experiments in Hele-Shaw cells [11]. In this paper we compare them with average profiles of DLA clusters.

Our first method for generating DBM in a channel is to use iterated conformal maps. The conformal mapping method for the radial case is described in Refs. [12,13]. For radial DLA, a map is created from the unit circle in the w (''mathematical'') plane to the unit circle with a bump at a randomly chosen angle in the physical plane; the composition of such maps is a map from the unit circle to the DLA cluster. To produce DBM clusters, instead of choosing the angles at random, we use a Monte Carlo method to select bump sites with the correct distribution [13].

To adapt this method to a channel, we modify the map of Stepanov and Levitov [14] for both periodic and reflective boundary conditions by requiring the map to be symmetric about the real axis. The map is given by

$$f_{\Lambda,\theta}(w)=\ln[g^{-1}\{\tilde{f}_{\Lambda}(g(w))\}], \tag{1}$$

where $g(w)=(w-1)/(w+1)$ is a map from the unit circle to the imaginary axis, and from the exterior of the unit circle to the positive-real half plane. The function

$$\tilde{f}_{\Lambda}(w)=\frac{w+\gamma\sqrt{(w-xi)^2+\Lambda^2}+\gamma\sqrt{(w+xi)^2+\Lambda^2}}{1+\gamma\sqrt{(1-xi)^2+\Lambda^2}+\gamma\sqrt{(1+xi)^2+\Lambda^2}} \tag{2}$$

adds two bumps at symmetric points $x'i$ and $-x'i$. The denominator in Eq. (2) forces $\tilde{f}_{\Lambda}(w)$ to map $w=1$ to 1, so that $f_{\Lambda,\theta}(w)$ maps ∞ to ∞. The parameter Λ controls the size of the bump and γ controls the aspect ratio of the bump. Since $g(w)$ maps -1 to ∞, we choose θ at random between 0 and π; and for $\theta>\pi/2$, $f_{\Lambda,\theta}(w)$ becomes

$$f_{\Lambda,\theta}(w)=-\overline{g^{-1}[\tilde{f}_{\Lambda}(g(-\bar{w}))]}, \tag{3}$$

where the bar denotes complex conjugation.

The actual bump positions are not at $\pm xi$, but are off by a small factor determined by x and Λ. The bump size is also dependent on x and Λ. In order to get bumps at angle θ, $\tilde{f}_{\Lambda}$ must place bumps at $g(e^{\pm i\theta})=\sin\theta/(1+\cos\theta)i$. We do this by an approximation method. To keep all the particles in the cluster of the same size, the bump size on the unit circle is varied according to the first derivative of the composite conformal map in the original version of the conformal map technique [12]. This assumes that the higher order derivatives are negligible, which is not true deep inside a fjord. Thus particles added in a fjord can end up being very large and sometimes can partially fill the channel. To combat this effect, we measure the bump area at each step, and iteratively correct the size parameter Λ if the area is outside of a preset tolerance (10% for the results in this paper); compare Ref. [14].

*Electronic address: e.somfai@warwick.ac.uk

While conformal mapping allows one to grow DBM for any η, and directly produces a conformal map for the cluster boundary, it is computationally intensive. A more efficient numerical algorithm for generating off-lattice DLA (that is, $\eta=1$) is a simple adaptation of hierarchical maps [15] to channel geometry. This method enables close to linear dependence of computing resources on cluster size. We used in total 1.7×10^{11} particles for the dimension calculations and (including probes) 4×10^{11} particles for the average profile.

Both periodic and reflective boundary conditions have been implemented on the sides of the channel (the periodic boundary condition is sometimes referred to as ''cylindrical''). The reflective boundary conditions are achieved as above: the cluster is grown in a channel of double width and periodic boundary conditions, and for each deposited particle we deposit also its mirror image. At the end one of the images was discarded. By the conventions used in this paper the channel is given by the range $-w/2<y<w/2$ and the clusters grow (macroscopically) in the positive x direction.

Fractal dimension of channel DLA. The fractal dimension is measured through the density. The average density scales with the width w of the channel, with exponent given by the codimension:

$$\rho(w)\sim w^{D-2}. \tag{4}$$

To avoid transients, we discarded the first and last $3w$ long section of the clusters and measured the density (number of particle centers per area) on the remaining middle section.

We generated clusters of 8×10^6–32×10^6 particles in channels of width $w=50,100,200,500,1000,2000,5000$ particle diameters. For each width the number of clusters grown ranged from a few hundred to a few thousand, with more and larger clusters necessary for large widths, to achieve comparable statistical confidence in the average density.

Figure 1 shows the width w dependence of the effective fractal dimension $D_{\rm eff}=2+d\ln\rho/d\ln w$. The fractal dimension tends to $D=1.712\pm0.002$, independent of the choice of boundary conditions. Off-lattice noise reduction [16] does not change the dimension, but accelerates the convergence to its asymptotic value.

Average profile. Analytical solutions for unbranched Laplacian growth in a channel with reflective boundary conditions have been known for a long time. One can find solutions which translate a fixed profile along the channel in time. In the absence of surface tension, these solutions form a one-parameter family, called Saffman-Taylor (ST) fingers [10]. They are parametrized by the asymptotic ratio λ of the widths of the finger ($w_{\rm finger}$) and the channel (w), and have the profile

$$x(y)=\frac{w(1-\lambda)}{2\pi}\ln\left[\frac{1}{2}\left(1+\cos\frac{2\pi y}{\lambda w}\right)\right]. \tag{5}$$

Of these solutions, $\lambda=1/2$ is the most important because in related experiments [10] this profile has been observed in the limit of vanishing surface tension. Analytical calculations [18–20] show that surface tension—a singular perturbation—selects a discrete set of finger solutions (only one of which is linearly stable), which all converge to the $\lambda=1/2$ ST finger in the limit of zero surface tension.

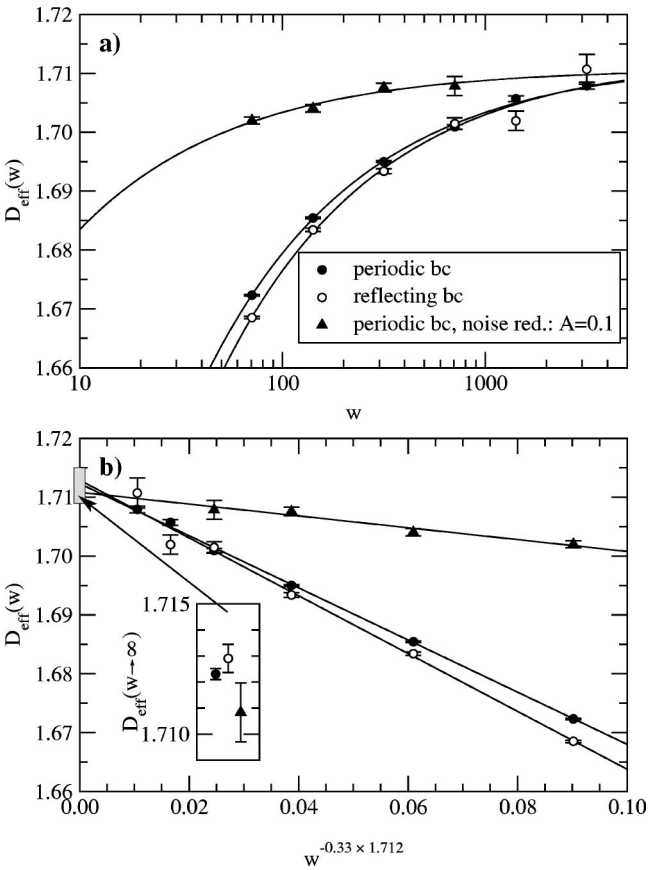

FIG. 1. (a) The (effective) fractal dimension as a function of channel width w. Circles correspond to the original model with periodic or reflecting boundary conditions, the triangles are made with off-lattice noise reduction [16]. For the three cases the ensemble size (and therefore the statistical uncertainty) was different. The curves correspond to the fitted lines in the (b) panel. (b) The finite size scaling plot of the same quantities, see Ref. [17]. Inset: All data is consistent in the $w\to\infty$ extrapolation with the dimension $D=1.712\pm0.002$. (In the inset the data is shifted horizontally for clarity.)

It has been suggested [21] that the $\lambda=1/2$ ST-finger solution also models the average profile both of the unstable (highly branched) Hele-Shaw fingering and of the DLA growth in a channel with the corresponding reflective boundary conditions. The profile was defined as a level set of the ensemble averaged mass density, and for the experimental Hele-Shaw profiles half of the maximum level was used. For DLA growth it was later shown [22] that the level set at 0.5 maximum matches the width of $\lambda=0.56$, while the best match to the $\lambda=1/2$ profile came from the level set at 0.6 maximum. Outside that range the authors of Ref. [22] concluded they could match level sets only to finger widths but not to the full shape of any ST finger.

Here we use a different kind of finger averaging, which does not have any fitting parameter (e.g., height of level set), as follows. In the conformal map method, we directly average the map. That is, we choose a set of points on the unit circle in the mathematical plane and repeatedly map to the

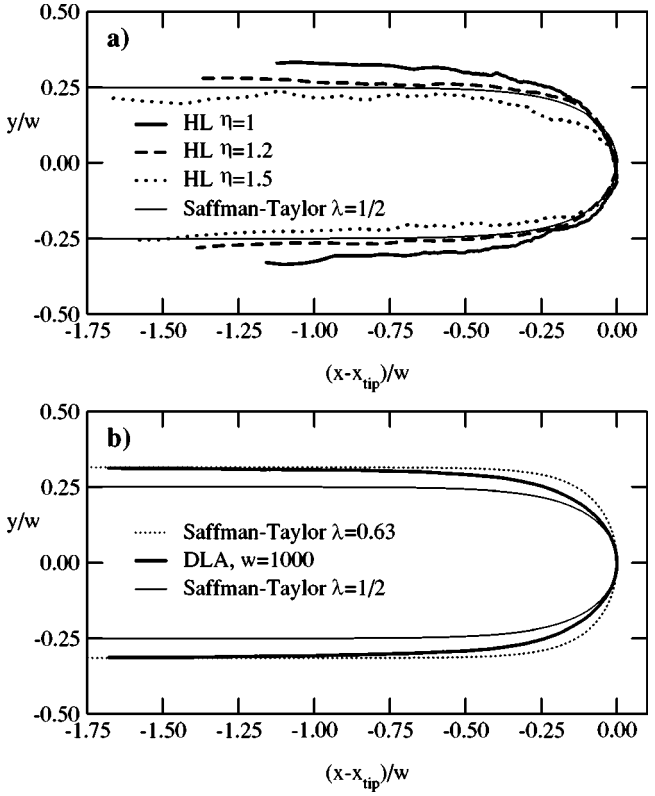

FIG. 2. (a) The average conformal map, generated with iterated conformal maps for $\eta=1$, 1.2, and 1.5. The profile for $\eta=1.2$ comes closest to the ST-finger solution for $\lambda=1/2$. (b) The average map of DLA clusters grown with random walking particles in a 1000 particle-diameter wide reflective channel. The profile does not follow any ST-finger solution.

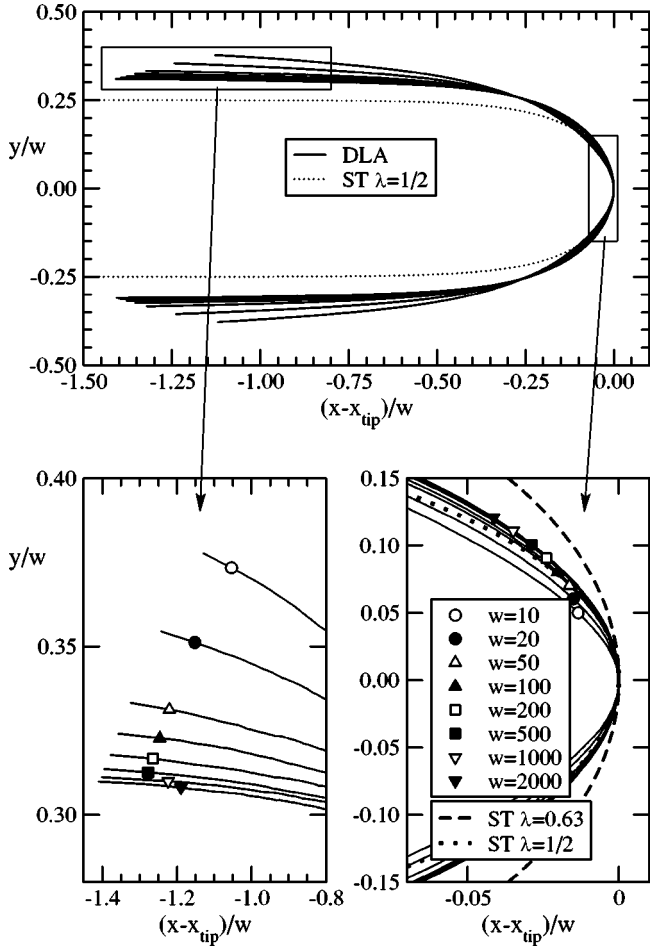

FIG. 3. The w dependence of the average conformal map, rescaled onto a unit wide channel. The tip and the tail are magnified on the bottom panels.

physical plane. The position of the image points averaged over the different maps, that is, over the different clusters that we have generated, is a reasonable alternative to the ensemble average of Refs. [21,22].

In Fig. 2(a) we show the average conformal map generated this way. We see that the average map for DLA, $\eta=1$, does not correspond to the ST result for $\lambda=1/2$, but we get a good match to it for the DBM growth at $\eta=1.2$. This is an interesting result, especially in the context of recently proposed equivalences between DBM models with generalized local spatial cutoff. In that framework [3,4] a highly ramified viscous finger with simple surface tension cutoff corresponds to standard (fixed size cutoff) DBM with $\eta\approx1.2$. Here we observe that the *nonbranching* ST-finger solution is very similar to the *conformal average* of DBM clusters of the same η.

To use DLA grown with random walking particles in a channel, we need only construct the conformal map from the complex unit circle to the perimeter of each cluster, and take the average of these maps, as above. The conformal map is obtained numerically by the following method [17]. We send M probe particles to the frozen cluster, record their impact position, and discard them. These points correspond to M uniformly distributed points on the unit circle. The landing

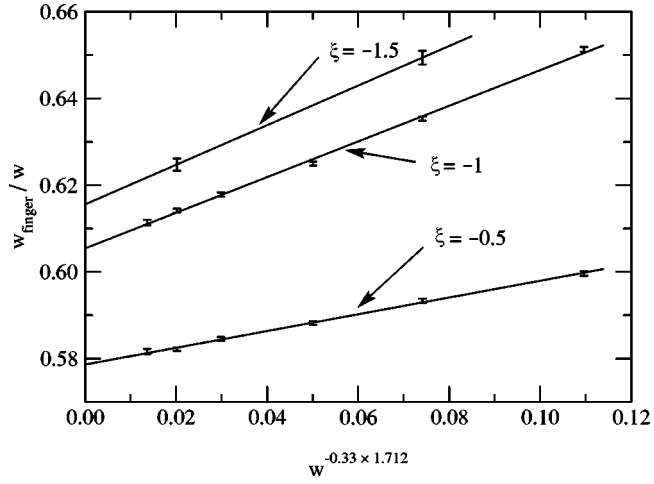

FIG. 4. Finite size scaling of the finger filling ratio $w_{\text{finger}}(\xi)/w$, measured at a few fixed ξ values. Only channels $50\leqslant w\leqslant2000$ were included in the fits. The finite size scaling gives the extrapolation $w\to\infty$. For the second extrapolation, $\xi\to-\infty$, we can only state that $w_{\text{finger}}/w\gtrsim0.62$.

positions of the probe particles are labeled topologically as one encounters them when tracking the perimeter of the cluster. Finally the mth point is assigned to the angle $2\pi m/M$ of the unit circle. This angle has an error of the order of $M^{-1/2}$, which vanishes for large M.

We measured the average conformal map on channels with reflective boundary conditions, widths ranging from 10 to 2000 particle diameters. For each width, we grew 10^5 short clusters (only about $10w$ long), and probed each with 10^5 test particles. In addition, for a few selected widths we probed 10^4 clusters with 10^6 probes each.

The average map for a wide channel generated this way is shown in Fig. 2(b). The curvature of the tip is consistent with that of the $\lambda=1/2$ ST finger (the measured curvature of the DLA profile for $w=1000$ or 2000 corresponds to $\lambda=0.51\pm0.03$). The asymptotic width, however, is larger. The average map significantly differs also from the ST finger of matching asymptotic width.

The average conformal map, rescaled onto a unit wide channel, shows strong dependence on the channel width. This is shown in Fig. 3 as a function of reduced x position relative to the tip, $\xi=(x-x_{\mathrm{tip}})/w$. Details of the tip and tail regions show that these are clearly not consistent with a common asymptotic ST-finger shape.

We performed a finite size scaling on the w dependence of the finger width. The filling ratio of the finger $w_{\mathrm{finger}}/w=[y_+(x)-y_-(x)]/w$ was measured at selected ξ values: $\xi=-0.5$, -1, and -1.5, and is plotted in Fig. 4. The finite size scaling exponent was found to be $\nu=0.33$, same as for other quantities [17,16]. The most interesting is the second extrapolation: $\xi\to-\infty$. We only have three points for this, so it is only reasonable to give a lower bound: $w_{\mathrm{finger}}/w\gtrsim0.62$.

In summary, using large scale random walker based simulations we have shown that the fractal dimension of DLA in a channel—with either periodic or reflective boundary conditions—is the same as in radial geometry. This is a great simplification compared to earlier claims of boundary condition (geometry) dependent fractal dimension. Second, using both iterated conformal maps and random walker based simulations, we measured the average profile of the clusters, defined by the average conformal map, and compared them to ST-finger solutions of the corresponding continuum problem. The averaged DLA profile is reminiscent but distinct from the ST fingers, while the average profile of DBM clusters with $\eta=1.2$ are rather similar to the ST finger with $\lambda=1/2$.

We are indebted to Dave Kessler for the suggestion of measuring the average conformal map. This research was supported by the EC under Contract No. HPMF-CT-2000-00800. The computing facilities were provided by the Center for Scientific Computing of the University of Warwick, with support from the JREI.

[1] T.A. Witten and L.M. Sander, Phys. Rev. Lett. **47**, 1400 (1981).
[2] L. Niemeyer, L. Pietronero, and H.J. Wiesmann, Phys. Rev. Lett. **52**, 1033 (1984).
[3] R.C. Ball and E. Somfai, Phys. Rev. Lett. **89**, 135503 (2002).
[4] R.C. Ball and E. Somfai, Phys. Rev. E **67**, 021401 (2003).
[5] P. Meakin and F. Family, Phys. Rev. A **34**, 2558 (1986).
[6] F. Argoul, A. Arneodo, G. Grasseau, and H.L. Swinney, Phys. Rev. Lett. **61**, 2558 (1988).
[7] C. Evertsz, Phys. Rev. A **41**, 1830 (1990).
[8] B. Kol and A. Aharony, Phys. Rev. E **62**, 2531 (2000).
[9] B. Kol and A. Aharony, Phys. Rev. E **63**, 046117 (2001).
[10] P.G. Saffman and G. Taylor, Proc. R. Soc. London, Ser. A **245**, 312 (1958).
[11] H. Thome, M. Rabaud, V. Hakim, and Y. Couder, Phys. Fluids A **1**, 224 (1989).
[12] M.B. Hastings and L.S. Levitov, Physica D **116**, 244 (1998).
[13] M.B. Hastings, Phys. Rev. Lett. **87**, 175502 (2001).
[14] M.G. Stepanov and L.S. Levitov, Phys. Rev. E **63**, 061102 (2001).
[15] R.C. Ball and R.M. Brady, J. Phys. A **18**, L809 (1985).
[16] R.C. Ball, N.E. Bowler, L.M. Sander, and E. Somfai, Phys. Rev. E **66**, 026109 (2002).
[17] E. Somfai, L.M. Sander, and R.C. Ball, Phys. Rev. Lett. **83**, 5523 (1999).
[18] R. Combescot, T. Dombre, V. Hakim, Y. Pomeau, and A. Pumir, Phys. Rev. Lett. **56**, 2036 (1986).
[19] B.I. Shraiman, Phys. Rev. Lett. **56**, 2028 (1986).
[20] D.C. Hong and J.S. Langer, Phys. Rev. Lett. **56**, 2032 (1986).
[21] A. Arneodo, Y. Couder, G. Grasseau, V. Hakim, and M. Rabaud, Phys. Rev. Lett. **63**, 984 (1989).
[22] A. Arneodo, J. Elezgaray, M. Tabard, and F. Tallet, Phys. Rev. E **53**, 6200 (1996).